

## **Engineering the NiO/CeO<sub>2</sub> interface to enhance the catalytic performance for CO oxidation**

Weixin Zou,<sup>a,b†</sup> Chengyan Ge,<sup>c†</sup> Minyue Lu,<sup>a,b</sup> Shiguo Wu,<sup>a,b</sup> Yongzheng

Wang,<sup>a</sup> Jingfang Sun,<sup>b</sup> Yu Pu,<sup>a</sup> Changjin Tang,<sup>a,b</sup> Fei Gao,<sup>\*a,b</sup> Lin

Dong<sup>\*a,b</sup>

<sup>a</sup> Key Laboratory of Mesoscopic Chemistry of MOE, School of Chemistry and Chemical Engineering, Nanjing University, Nanjing 210093, PR China

<sup>b</sup> Jiangsu Key Laboratory of Vehicle Emissions Control, Center of Modern Analysis, Nanjing University, Nanjing 210093, PR China

<sup>c</sup> School of Chemistry and Chemical Engineering, Yancheng Institute of Technology, Yanchen 224051, PR China

† These authors contribute equally.

### **Corresponding Author**

\*E-mail: gaofei@nju.edu.cn, donglin@nju.edu.cn Tel: +86-25-83592290 Fax: +86-

25-83317761

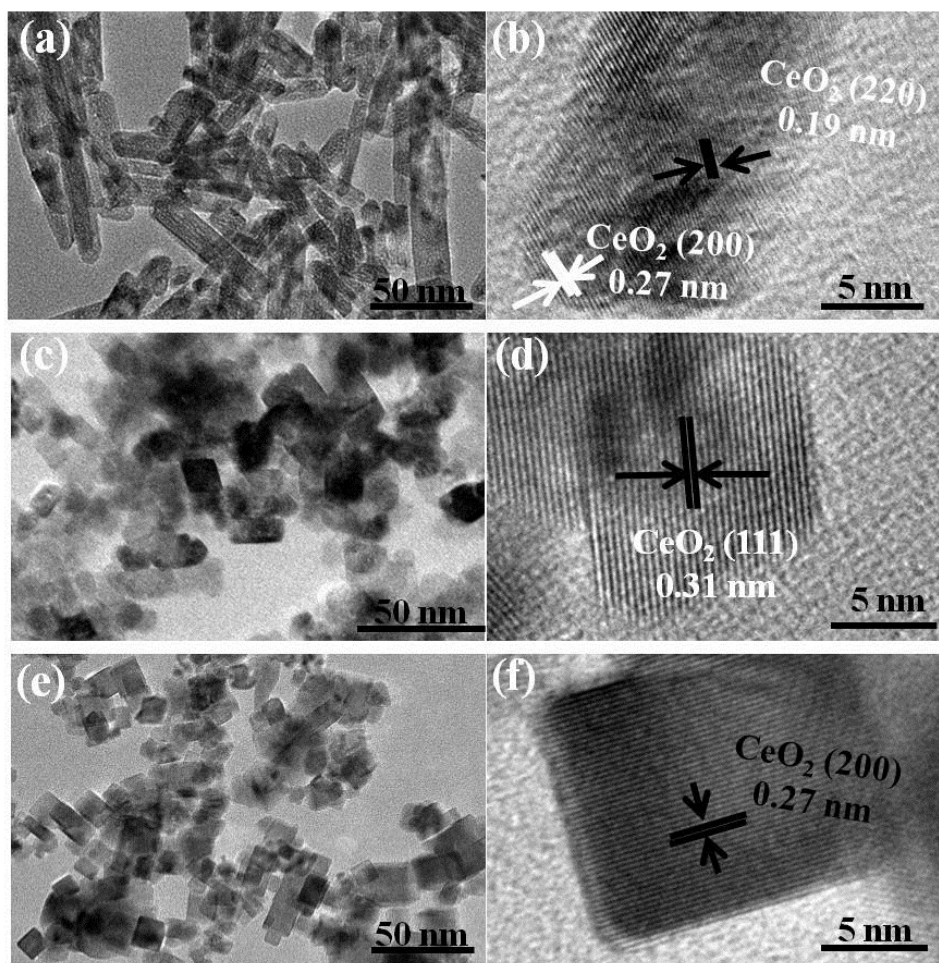


Figure S1. TEM and HRTEM images of CeO<sub>2</sub> (a, b) nanorod; (c, d) nanooctahedron; (e, f) nanocube.

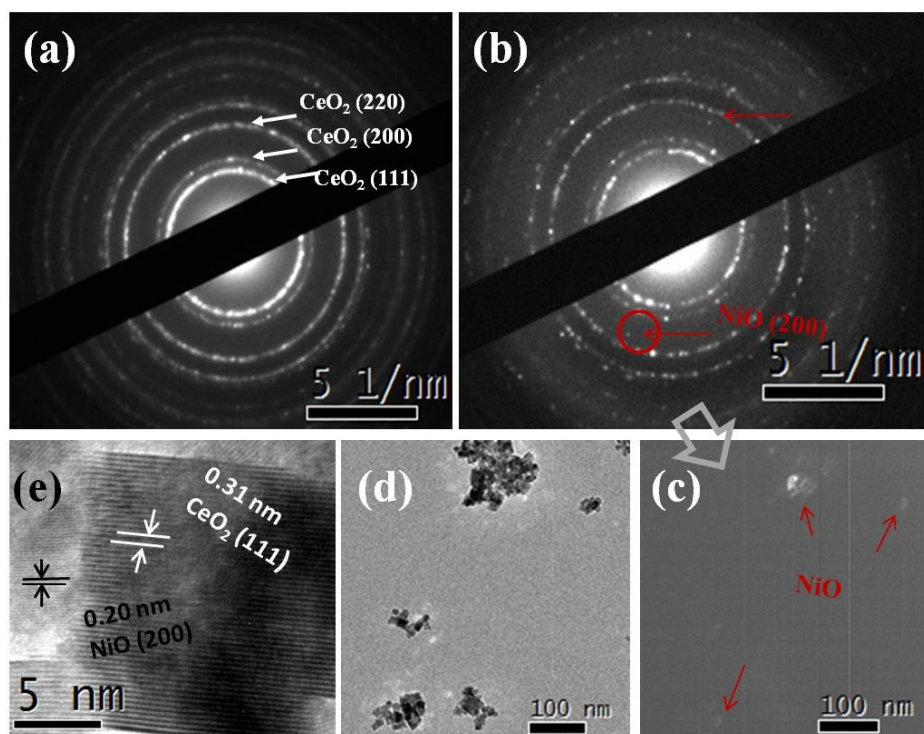


Figure S2. Electron diffraction patterns of (a) CeO<sub>2</sub> octahedron, (b) Ni/CeO<sub>2</sub> octahedron; (c) the corresponding dark field image of white spot in the red circle; (d) the corresponding bright field image; (e) the HRTEM image of Ni/CeO<sub>2</sub> octahedron.

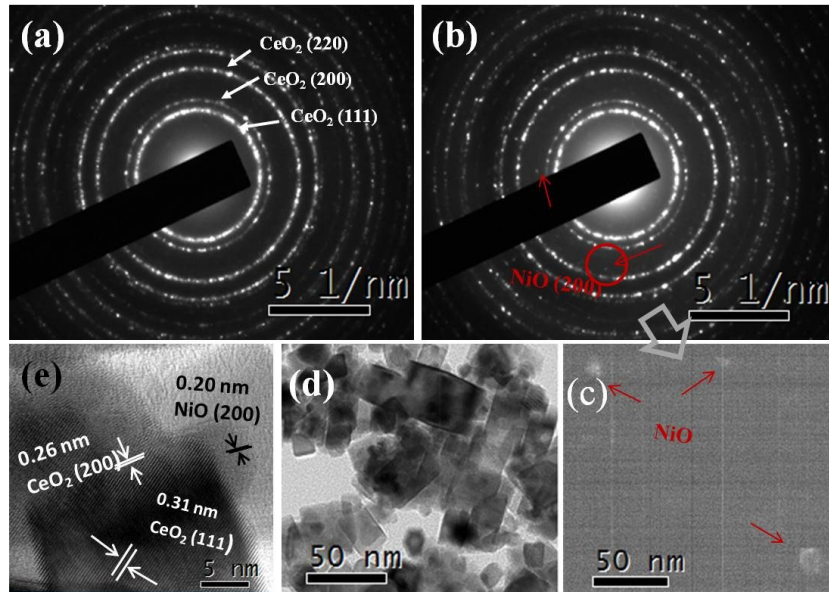


Figure S3. Electron diffraction patterns of (a) CeO<sub>2</sub> cube, (b) Ni/CeO<sub>2</sub> cube; (c) the corresponding dark field image of white spot in the red circle; (d) the corresponding bright field image; (e) the HRTEM image of Ni/CeO<sub>2</sub> cube.

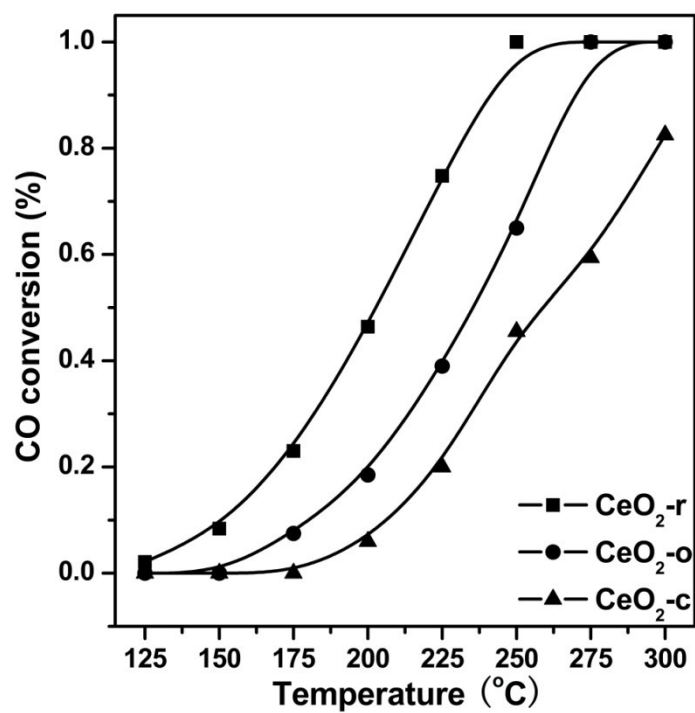


Figure S4. CO conversion over CeO<sub>2</sub> catalysts with different shapes.

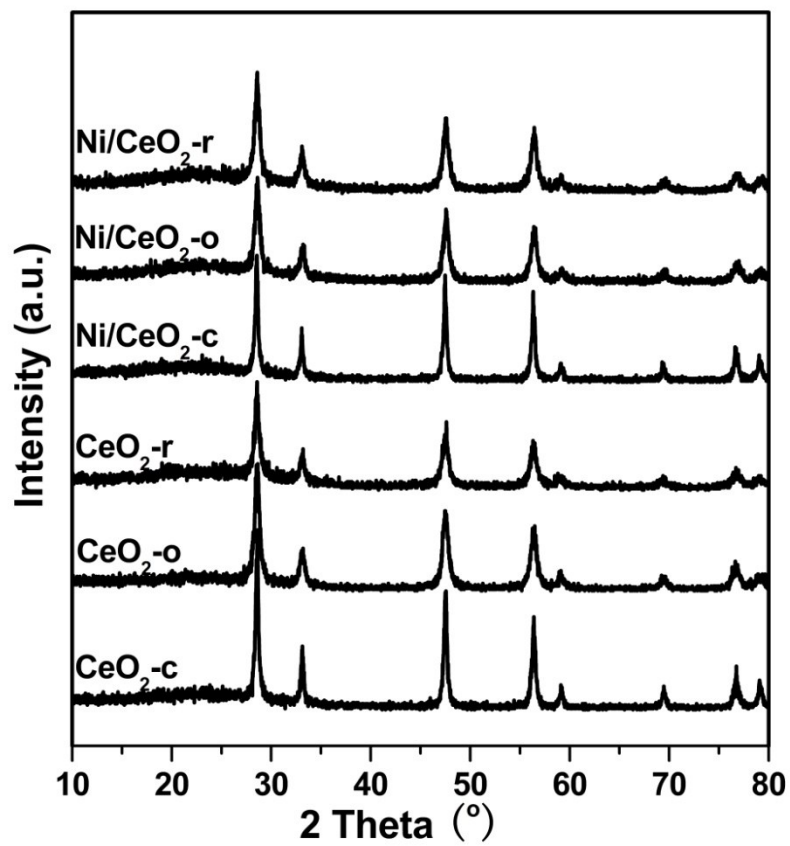


Figure S5. XRD patterns of Ni/CeO<sub>2</sub> and CeO<sub>2</sub> samples with different shapes.

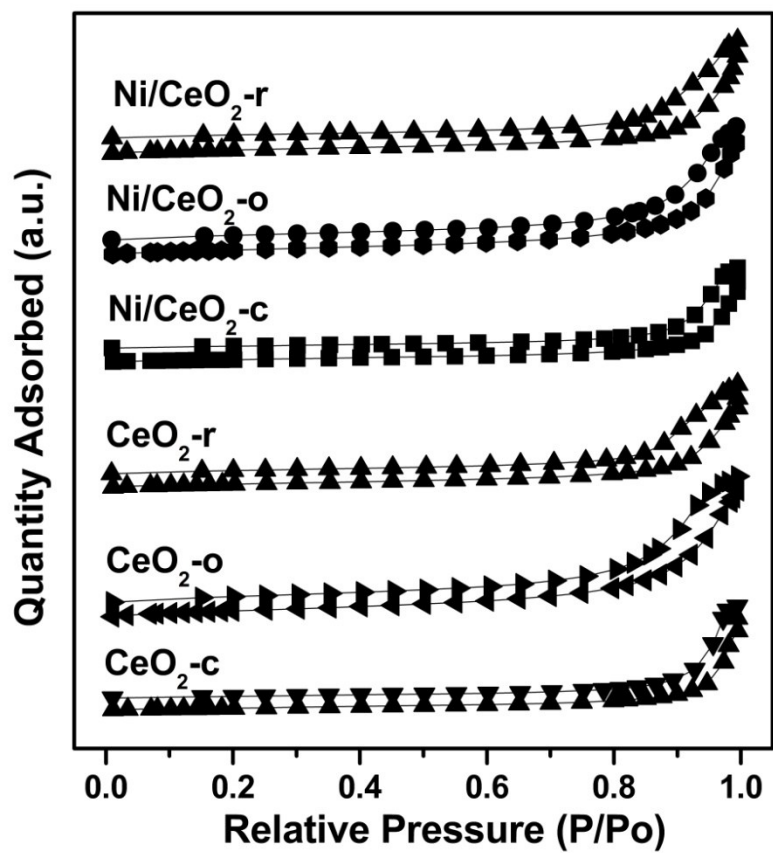


Figure S6. N<sub>2</sub> adsorption–desorption isotherms of Ni/CeO<sub>2</sub> and CeO<sub>2</sub> samples with different shapes.

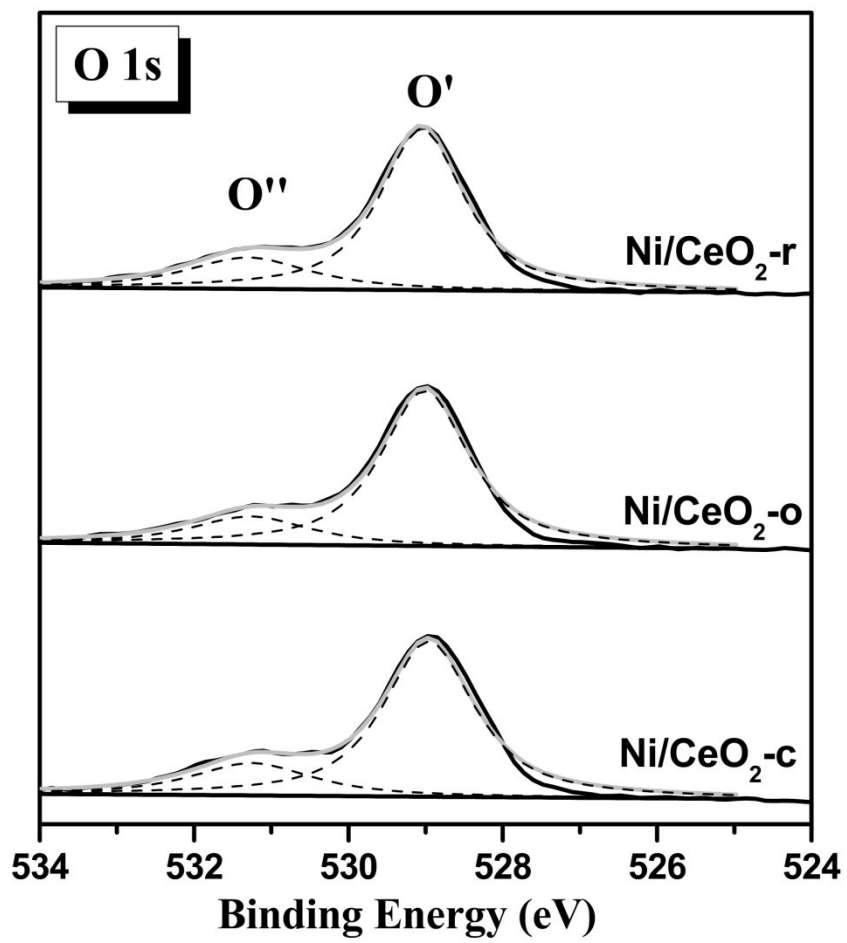


Figure S7. XPS spectra of O 1s over Ni/CeO<sub>2</sub> catalysts with different shapes.



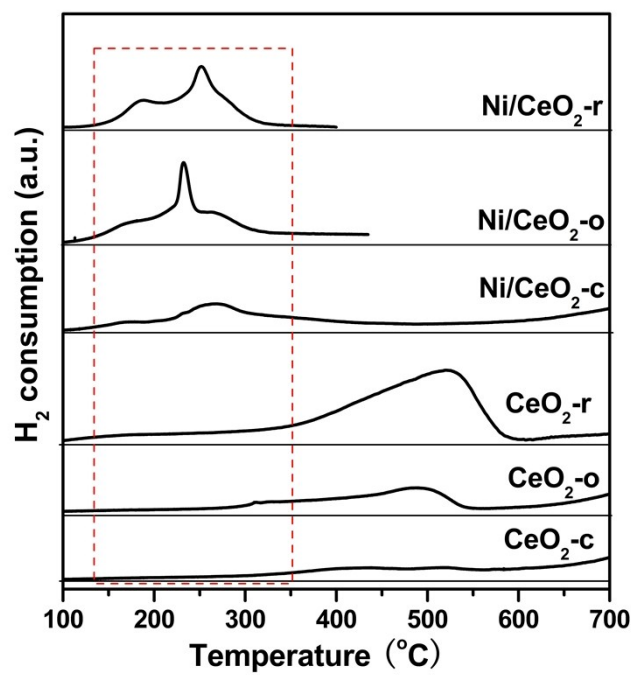


Figure S8. H<sub>2</sub>-TPR profiles of Ni/CeO<sub>2</sub> and CeO<sub>2</sub> with different shapes.

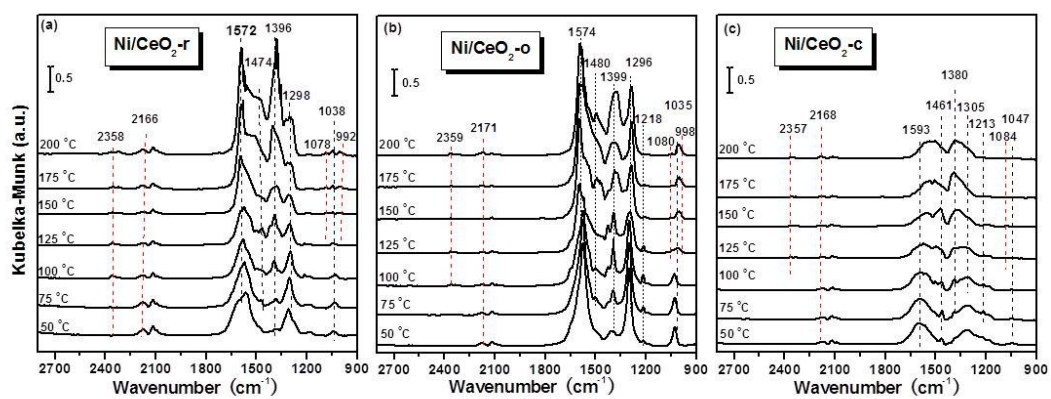


Figure S9. *In-situ* CO-adsorption DRIFTS of Ni/CeO<sub>2</sub> catalysts with different shapes.

Table S1. Surface area, crystallite size, lattice parameter,  $I_{605+1172}/I_{460}$  in Raman spectra and turnover frequency ( $TOF_{CO}$ ) at 120 °C of Ni/CeO<sub>2</sub> and CeO<sub>2</sub> samples, respectively.

Samples	$S_{BET}$ (m <sup>2</sup> /g)	Grain size (nm)	Lattice parameter (Å)	$I_{605+1172}/I_{460}$ 0	$TOF_{CO}^a$ (h <sup>-1</sup> )
Ni/CeO <sub>2</sub> -r	64	12.8	5.4052	0.32	35.2
Ni/CeO <sub>2</sub> -o	84	16.6	5.4050	0.21	10.1
Ni/CeO <sub>2</sub> -c	30	24.8	5.4011	0.12	0.5
CeO <sub>2</sub> -r	66	11.5	5.4133	0.054	
CeO <sub>2</sub> -o	85	12.9	5.4064	0.051	
CeO <sub>2</sub> -c	32	24.6	5.4022	0.046	

a:  $TOF_{CO} = P \cdot Sv \cdot C_{CO} \cdot X_{CO} / R \cdot T \cdot C_{Ni}$ , in which P was the atmospheric pressure,  $C_{CO}$  was the molar CO concentration at the inlet, Sv was the space velocity, X was the CO conversion and  $C_{Ni}$  was the molar concentration of surface Ni atoms determined by XPS.